Is the Photoinduced Isomerization in Retinal Protonated Schiff Bases a Single- or Double-Torsional Process?†

Jaroslaw J. Szymczak,*,‡ Mario Barbatti,‡ and Hans Lischka*,‡,§

Institute for Theoretical Chemistry, University of Vienna, Waehringerstrasse 17, A-1090, Vienna, Austria, and Institute of Organic Chemistry and Biochemistry, Academy of Sciences of the Czech Republic, Flemingovo nam. 2, CZ-16610 Prague 6, Czech Republic

Received: April 10, 2009; Revised Manuscript Received: June 25, 2009

Nonadiabatic photodynamical simulations are presented for the all-trans and 5-cis isomers of the hepta-3,5,7-trieniminium cation (PSB4) with the goal of characterizing the types of torsional modes occurring in the cis-trans isomerization processes in retinal protonated Schiff base (RPSB), the rhodopsin and bacteriorhodopsin chropomhore. Steric hindrance of these processes due to environmental effects have been modeled by imposing different sets of mechanical restrictions on PSB4 and studying its response in the photodynamics. Both the mechanism toward the conical intersection and the initial phase of the hot ground state dynamics has been studied in detail. A total of 600 trajectories have been computed using a complete active space self-consistent field wave function. Careful comparison with higher level methods has been made in order to verify the accuracy of the results. The most important mechanism driving restricted PSB4 isomerization in the excited state is characterized by two concerted twist motions (bipedal and closely related to it nonrigid bipedal) from which only one torsion tends to be continued during the relaxation into the ground state. The one-bond-flip is found to be important for the trans isomer as well. The main isomerization trend is a torsion around C_5C_6 (equivalent to $C_{11}C_{12}$ in RPSB) in the case of the cis isomer and around C_3C_4 ($C_{13}C_{14}$ in RPSB) in the case of the trans isomer. The simulations show an initial 70 fs relaxation into twisted regions and give an average internal conversion time of 130−140 fs, timings that are fully compatible with the general picture described by femtosecond transient absorption spectroscopic studies.

Introduction

Photoinduced isomerization is a widely discussed topic affecting a large variety of systems of chemical and biological interest. One particularly important subject in this field concerns the cis-trans isomerization of photoexcited retinal protonated Schiff base (RPSB). RPSB is the chromophore of a family of rhodopsins and plays a key role in several biological processes. For example, the cis-trans photoisomerization of 11-cis RPSB, the chromophore of rhodopsin (Rh),[1−5] is the primary step in the process of vision, while a trans-cis photoisomerization (all-trans RPSB to 13-cis RPSB) in bacteriorhodopsin (bR)[6,7] is the driving force for a proton pump through cell membranes of *Halobacterium salinarium*. In both cases, the change in the protein conformation is triggered by the light-induced isomerization of RPSB that is bound to the protein by a Schiff base link. These photoisomerization processes[8,9] belong to the fastest photochemical reactions in nature[1] and have been studied extensively in experimental[10−13] and theoretical investigations.[14−31]

The large size of RPSB and the multireference character of the electronic wave function make high level accurate calculations very difficult to perform, especially when dynamics simulations are intended. Because of this limitation, the photochemical properties of RPSB have been studied theoretically mostly by simulation of model systems. For that purpose, the penta-3,5-dieniminium cation (PSB3), one representative of the family of protonated Schiff bases $CH_2(CH)_{2n-2}NH_2^+$ (PSBn), has been chosen as the simplest RPSB model in several investigations.[32−43] The photochemistry of PSB3 has been addressed mostly by performing static calculations on excited-state energy surfaces, with determination of stationary points, conical intersections[32,37,44] and minimum energy paths.[34,35,38,39,42] Most of these investigations dealt with the isolated species omitting any further restrictions. In this case, the photoisomerization proceeds in a relatively simple way by in-plane skeletal relaxation followed by torsion around the central C═C bond. This motion is termed one-bond-flip (OBF) (see Figure 1a).[10,45,46] This picture is corroborated by several nonadiabatic dynamics simulations.[33,40,41] PSB3 is, however, relatively small and the limited number of possible isomerization sites result predominantly in the rotation around the central double bond. Another important limitation of the unrestricted RPSB models is related to the spatial requirements for the cis-trans isomerization, which together with electrostatic effects[47] constitute essential aspects for the isomerization within the protein pocket. Only few studies have been carried out beyond vertical excitations with environmental effects taken into account.[17,32,44,45,47−50]

The OBF is the simplest way of performing nonrestricted isomerization; however, it is supposed to be strongly inhibited in the protein environment because of spatial limitations. Several mechanisms of the restricted photoisomerization have been discussed in the literature. One of the proposed alternatives to the OBF mechanism is the bicycle-pedal motion (BP, Figure 1c), which consists of the simultaneous torsion of two neighboring formal double-bonds with rigid formal single bond connection. This motion has been introduced by Warshel[27] based on dynamics simulations of RPSB with spatial constrains using a

† Part of the "Walter Thiel Festschrift".

* To whom correspondence should be addressed. E-mail: (J.J.S.) jaroslaw.szymczak@univie.ac.at; (H.S.) hans.lischka@univie.ac.at.

‡ University of Vienna.

§ Academy of Sciences of the Czech Republic.

10.1021/jp903329j CCC: $40.75
Published on Web 08/04/2009

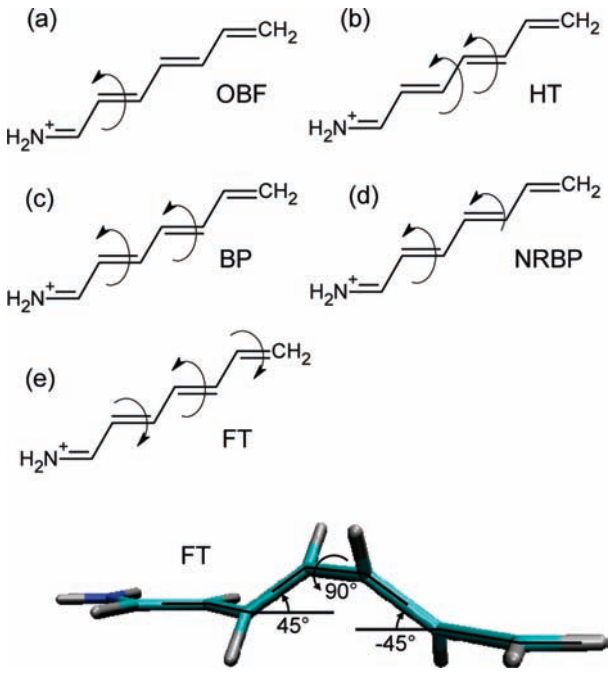

Figure 1. Torsional motions involved in the main isomerization mechanisms: (a) OBF; (b) HT; (c) BP; (d) NRBP; (e) FT.

combination of force field and Pariser−Parr−Pople methods.[51] Later on, Warshel and Barboy[28] noted also another isomerization mechanism similar to the BP where one of the torsions proceeded only partially (slower or starting slightly later). We refer to this mechanism as nonrigid BP (NRBP, Figure 1d) because of its resemblance to the bicycle pedal motion where one of the pedals is somewhat "loose". This kind of mechanism has been described also in recent work by Schapiro et al.[15] and by Hayashi et al.[17] The structure of the conical intersection related to this type of the mechanism has been recently reported in quantum mechanics/molecular mechanics (QM/MM) investigations by Andruniow et al.[26] and in a high-level one-trajectory dynamics study of RPSB performed by Frutos et al.[20] Another way of performing a cis-trans isomerization consisted of a concerted torsion or hula-twist (HT, Figure 1b) proposed by Liu and Asato.[52] This process consists of simultaneous torsion of two adjacent bonds followed by skeletal relaxation. Sumita and Saito suggested[39] that HT is more likely to be observed in heavily restricted systems. However, recent surface-hopping dynamics studies[40] using mass restrictions at the terminal hydrogen atoms of PSB3 do not show any evidence supporting this suggestion. In addition to the just-mentioned mechanisms a new type of volume-conserving mechanism has been proposed in ref 40, the folding table (FT; see Figure 1e). It can be described as a combination of three torsions with the main one accompanied by two partial or half-torsions around formal neighboring double bonds. These partial rotations are located at both sides of the main torsion and are separated from it by a dihedral angle that does not change during isomerization. The simulations showed that the significance of this motion increases with the extent of geometrical restrictions imposed.

In the present work, the photodynamics of hepta-3,5,7-trieniminium cation (PSB4) is investigated by performing extended on-the-fly surface hopping dynamics calculations. As the results show, this compound shows a significantly enhanced torsional variability while keeping the computational effort for the on-the-fly hopping calculations manageable so that a good statistics within the framework of ab initio approaches can be achieved. As performed in our previous work,[40] mechanical restrictions corresponding to the protein link on one PSB4 end and representing the remaining RPSB molecule on the other were applied. Two isomers of PSB4 (5-cis-PSB4, denoted later on as cis-PSB4, and all-trans-PSB4, denoted as trans-PSB4) were investigated in order to model the rhodopsin and bacteriorhodopsin chromophore, respectively. The dynamics results for doubly restricted PSB4 are compared to time-dependent femtosecond-resolved experiments[4,10,53,54] and the implications for RPSB isomerization are discussed.

In total, 600 trajectories have been simulated and the isomerization mechanisms before and after the internal conversion have been classified. Since completely general rules for the structural classification of different torsional structures are applied, the present classification scheme is not restricted to the currently investigated system of protonated Schiff bases, but can also be used for any molecular chain involved in cis-trans isomerization. In this work a full nonadiabatic dynamics in the framework of Tully's fewest switches surface hopping approach[55,56] is reported, which should improve the treatment of the nonadiabatic transitions in comparison to simpler surface-hopping algorithms employed in other PSB studies.[16,17]

Computational Details

Electronic Structure and Dynamics Methods. Complete active space self-consistent field (CASSCF) calculations were performed for PSB4. Eight electrons were included in the calculations within an active space consisting of eight orbitals (four π and the corresponding four π^* orbitals) and averaged over two states [SA-2-CASSCF(8,8)]. For the calculations of the vertical excitation energies and conical intersections (minima on the crossing seam (MXS)) multireference configuration interaction (MRCI) calculations were performed also. For the MRCI calculations a CAS(6,6) reference space was chosen denoted as MRCI(6,6) where a natural orbital occupation criterion was used to move the lowest CASSCF orbital (occupation 1.97) into the doubly occupied space and the highest one (occupation less than 0.05) into the virtual space. The CI expansion included either all single and double excitations (MR-CISD) or only single excitations (MR-CIS) with respect to the CAS(6,6) reference space. In the case of MR-CISD, the generalized interacting space restriction[57] was adopted. Higher-order excitation effects are accounted for by the Davidson correction (+Q) for single-point calculations.[58−60] The static calculations (vertical excitation energies and potential energy curves) were performed with the 6-31G* and 3-21G basis sets.[61,62] The former basis set was used to verify the application of the smaller one in the dynamics simulations.

Mixed quantum-classical dynamics simulations were performed using Tully's surface hopping approach.[55,56] The nuclear motion was obtained by solving Newton's equations on the Born−Oppenheimer potential energy surface. Energies, energy gradients and nonadiabatic coupling vectors were computed on-the-fly. The integration of the classical equations is performed by means of the velocity−Verlet algorithm[63] in time-steps of 0.5 fs. The total simulation time was 200 fs. The time-dependent wave function was expanded in the adiabatic representation and the time-dependent Schrödinger equation was integrated using the fifth-order Butcher algorithm.[64] In order to further improve the numerical integration of the electronic time-dependent Schrödinger equation, a smaller time step $\Delta t' = \Delta t/m_s$ ($m_s = 20$) is used with potential energies and nonadiabatic coupling vectors interpolated between t and $t + \Delta t$. The obtained time-dependent adiabatic populations were corrected for decoherence effects[65] ($\alpha = 0.1$ hartree) and used for computing the

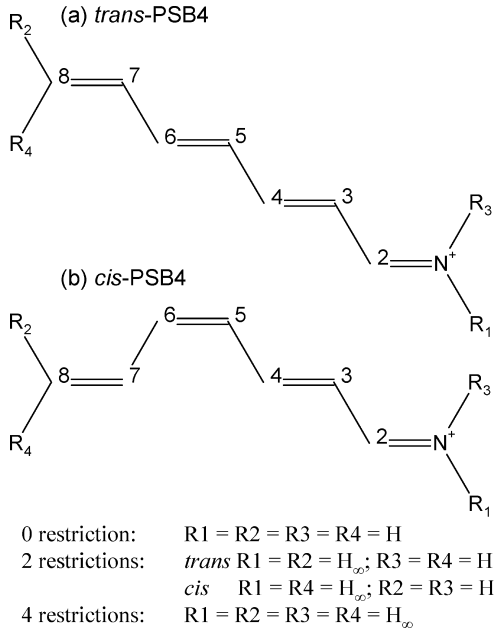

Figure 2. Numbering scheme for (a) trans- and (b) cis-PSB4 with indication of the restrictions employed in this work. H_∞ stands for hydrogen atom with increased isotopic mass.

surface-hopping probabilities for nonadiabatic transitions according to the fewest-switches algorithm[55,56] in the version proposed by Hammes-Schiffer and Tully.[66] At each time-step, a random event is used to decide whether the system will switch to another state. The momentum after frustrated hoppings was kept constant and after actual hoppings it was readjusted along the nonadiabatic coupling vector. The initial conditions for the simulated trajectories were generated by means of a ground-state Wigner distribution (0 K) by treating the nuclear coordinates and momenta within the quantum-harmonic-oscillator approximation. To sample the random initial geometries and velocities, normal modes and frequencies were computed for trans and cis isomers for each different set of restrictions.

As already mentioned above, in addition to the nonrestricted dynamics calculations, restricted simulations were performed. The restrictions were imposed by increasing the masses of the terminal hydrogen atoms. Two sets of restrictions were constructed. In the first set, the nuclear masses of the two hydrogen atoms (R_1 and R_4 in Figure 2, later on denoted as restricted hydrogens) were modified. The choice of two restricted hydrogen atoms is meant to model the situation where the one at the nitrogen end represents the binding of PSB4 to the protein (Lys_{216} in bR for trans isomer, or Lys_{296} in Rh for cis isomer) whereas the other one stands for the rest of the RPSB chain. For all cases, a mass of 1000 amu was used. This choice practically fixes the positions of these hydrogen atoms during the dynamics. For the trans (cis) isomer, this mass gives the moment of inertia for torsion of R2 (R4) around the C_7C_8 bond similar to moment of inertia for torsion of the remaining RPSB chain. This mass restriction technique was previously successfully applied by Warshel[27] for the investigations of RPSB and in our previous investigations on the dynamics of PSB3 system[40] and on aminopyrimidine.[33,67] The advantage of this approach is that the restricted dynamics can be performed at the same computational cost of nonrestricted investigations. In the second set of restrictions, masses of 1000 au were assigned to all four terminal hydrogens. The 4-restricted PSB4 was investigated to understand the role of each isomerization mechanism with a systematic increase of restrictions.

TABLE 1: $\Delta\theta$ Patterns[a] Used for the Classification of Motions in PSB4

	dihedral angle change $\Delta\theta_i$						
	N−C2	C2−C3	C3−C4	C4−C5	C5−C6	C6−C7	C7−C8
OBF	a	a	a	a	c	a	a
FT	a	a	b	a	c	a	b
BP	a	a	c	a	c	a	a
NRBP	a	a	b	a	c	a	a
HT	a	a	c	c	a	a	a

[a] Ranges of torsional angles: a, $0° \le \Delta\theta < 30°$; b, $30° \le \Delta\theta < 60°$; c, $60° \le \Delta\theta \le 90°$.

A total of 600 trajectory calculations for investigated systems were performed (100 for the system with no, two, and four restrictions for both isomers of PSB4). The CASSCF and MR-CI calculations have been performed using the COLUMBUS program system[68−70] using the methods for analytic computation of gradient and nonadiabatic coupling vectors described in refs 58, and 71−74. The dynamics calculations were carried out by means of the program system NEWTON-X[75,76] using the quantum chemical data computed by COLUMBUS at each time step. For the automatic classification of the observed motions an analysis program was developed.

Algorithms for Data Analysis. The analysis of the dynamics is divided into two stages. The first stage concerns the motions leading to the conical intersection. They have been analyzed in terms of relative changes ($\Delta\theta_i$) of dihedral angles at the moment of the first hopping. The dihedral angles used in the analysis are defined along the PSB4 chain by the heavy atoms and, in case of terminal torsions, by inclusion of terminal hydrogen atoms. In the case of dynamics with two restrictions, hydrogen atoms that possess heavy masses were selected. On the basis of this selection, all geometries were classified according to their dihedral changes. Table 1 shows examples of $\Delta\theta_i$ patterns corresponding to each of the five types of isomerization mechanisms mentioned in the Introduction. Each $\Delta\theta_i$ value is assigned one of three ranges: *significant* (also denoted by the letter c) for $\Delta\theta_i$ larger than 60°, *partial* or "b" for $30° \le \Delta\theta_i \le 60°$ or *unchanged* ("a") for $0° \le \Delta\theta_i < 30°$. The OBF[10,45,46] is defined as the process for which there is only one *significant* change in a dihedral angle. The FT mechanism can be described as a combination of three torsions with the main central torsion accompanied by two *partial* torsions on both sides, separated on each side by one *unchanged* dihedral angle. The BP mechanism[27] is characterized by simultaneous *significant* changes of two dihedrals that are separated by one dihedral angle in between that stays *unchanged* during the motion. The NRBP mechanism[28] represents a case similar to BP, however the torsion around one of the bonds proceeds slower or starts later than the other, therefore results in a *partial* change of the corresponding dihedral angle. The last mechanism,[37,52,77] HT or concerted twist can be described as a simultaneous significant change of two adjoined dihedrals not accompanied by any other torsion.

The second stage of the torsional part of the dynamics, the behavior of the molecule after the hopping to the ground state, has been examined from two points of views. The first one concerns the continuation of the motion leading to the conical intersection and the second one its outcome in terms of the final product. For the first purpose, geometries were systematically checked 20 fs after the hopping for changes in the dihedral angles that correspond to torsions characteristic for the given type of motion. In the OBF case, for example, only the dihedral angle with *significant* change was checked. The motion is

TABLE 2: Relative Energies (eV) of Stationary Points and MXSs for Cis and Trans Isomers of PSB4[a]

		CASSCF		MR-CIS		MR-CISD		RICC2
geometry	state	6-31G*	3-21G	6-31G*	3-21G	6-31G*	3-21G	TZVP
				trans-PSB4				
S_0 min	S_1	4.00	4.09	3.60	3.62	3.82 [3.55]	3.83 [3.60]	3.47
S_1min	S_1	3.61	3.64	3.37	3.39	3.60 [3.43]	3.60 [3.35]	3.36
				cis-PSB4				
S_0 min	S_0	0.12	0.11	0.12	0.11	0.12 [0.12]	0.10 [0.10]	0.12
	S_1	4.07	4.17	3.66	3.70	3.89 [3.61]	3.91 [3.66]	3.51
S_1min	S_1	3.60	3.65	3.37	3.37		3.50 [3.42]	3.37
				MXS				
MXS cis-C_3C_4	S_0/S_1	2.65	2.61	2.58	2.49	2.52 [2.33]	2.41 [2.36]	
MXS trans-C_3C_4	S_0/S_1	2.56	2.51	2.49	2.39		2.32 [2.28]	
MXS C_5C_6	S_0/S_1	2.72	2.92	2.44	2.60		2.55 [2.69]	
MXS cis-BP	S_0/S_1	3.34	3.42	3.44	3.48	3.19 [3.00]	3.20 [3.12]	
MXS trans-BP	S_0/S_1	3.29	3.36	3.37	3.41		3.15 [3.07]	

[a] Geometries computed with CASSCF(8,8), MR-CIS(6,6) and MR-CISD(6,6) methods. MXS geometries optimized at CASSCF(8,8) level. The reference values of the trans-PSB4 ground state minimum are given in Hartrees (CASSCF, 6-31G* −325.174000, 3-21G −323.371040; MR-CIS, 6-31G* −325.277484, 3-21G −323.456071; MR-CISD, 6-31G* −325.964953 [−326.203368], 3-21G −323.931186 [−324.080914]; RICC2, TZVP −326.343351). In the case of MRCI calculations, the MXS energy is calculated as an average over the S_0 and S_1 energies computed at the CASSCF(8,8) geometries.

classified as continued or reversed if the change in the torsional angle is larger than $+\delta$ or smaller than $-\delta$, respectively. A value of 20° was chosen for δ. If this threshold is not reached within this time, the motion is examined again after 5 fs. The procedure is continued until 60 fs after the hopping, always trying to classify the motion after hopping either as continued or as reversed.

Independently, the final product of the photodecay is analyzed in terms of absolute values of all dihedral angles. A four-atom segment (bond) is considered as trans (ε) if the corresponding dihedral is in the range of 180 ± 60° or cis (ζ) if the angle fell into the range 0 ± 60°. A nonstandard notation is used for the classification of torsional angles around single and double bonds since individual bonds alter their bond character during the dynamics significantly. The $\varepsilon\varepsilon\varepsilon\varepsilon\varepsilon\varepsilon\varepsilon$ and $\varepsilon\varepsilon\varepsilon\varepsilon\zeta\varepsilon\varepsilon$ patterns, for example, correspond to the all-trans and to the 5-cis structures, respectively. It is expected that the application of such a final product analysis to be especially important for the restricted systems. Since the full relaxation is not allowed in the case of restricted motion, the excess energy can cause additional torsions, usually not observed in the case of the nonrestricted dynamics. Therefore, especially with 4-restricted PSB4 the straightforward continuation of the motion leading to the conical intersection need not result in the formation of the corresponding final product.

Results and Discussion

Investigation of the Potential Energy Surfaces. ***Description of the Minima, MXSs and Reaction Paths.*** The cis- and trans-PSB4 ground state minima show planar conformations. The vertical excitation energies are given in Table 2, footnote *a*. Full Cartesian coordinates computed at the CASSCF(8,8) level are collected in the Supporting Information (see the end of the text for more information). Investigations based on the minimum energy path approach applied to PSBn systems have shown[30,35] that the excited state dynamics of PSBn systems can be described by an initial planar skeletal relaxation followed by a torsional motion. Therefore, it is important to consider the geometry of the planarity-restricted S_1 minimum (S_1min) first. The main geometrical parameters are shown in Figure 3. For both isomers, the ground state shows a distinct alternation between single and double bonds. In the excited state, the C_3C_4 and C_5C_6 bonds are strongly elongated for both isomers becoming most likely to undergo torsional motions.[32] For detailed discussions of restricted planar relaxation and comparison between CASSCF and MR-CISD results see ref 32.

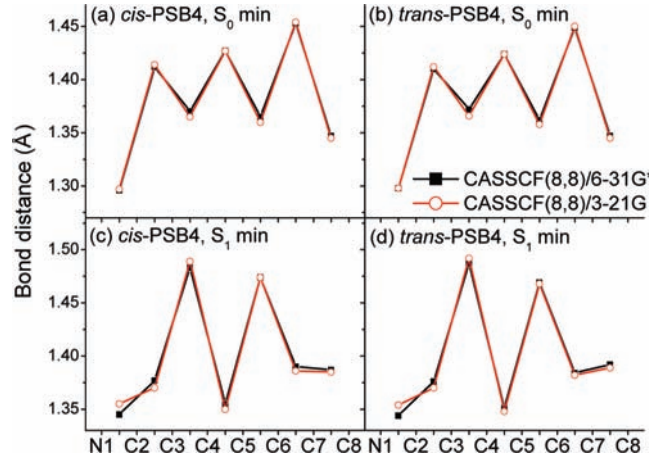

Figure 3. CN and CC bond lengths (see Figure 2 for numbering scheme) for the ground state (a and b) and S_1 minima (c and d) for cis- and trans-PSB4.

Each of the different isomerization mechanisms leads to a separate conical intersection in PSB4. Five minima on the crossing seam (MXS) have been determined (see Figure 4).

Their energies are collected in Table 2. The lowest energy MXSs correspond to the twist around the C_3C_4 bond (Figure 4a,b). The twist around the C_5C_6 bond produces another MXS close in energy to the previous ones. Its structure is shown in Figure 4c. The twist involving C_3C_4 and C_5C_6 leading to the BP mechanism, produces two MXSs (trans and cis) characterized in Figure 4d,e. Figure 4f shows a conical intersection for the FT mechanism, which occurred during the dynamics simulations. This conical intersection, however, is not a minimum on the crossing seam and upon optimization it relaxes into the MXS C_3C_4.

Reaction paths between the cis- and trans-S_1min geometry and the five MXSs are shown in Figure 5. They are obtained by means of linear interpolation of internal coordinates (LIIC). In all cases except one, the path to the MXS is barrierless. In the path between the trans-PSB4 and the MXS C_5C_6, there is a

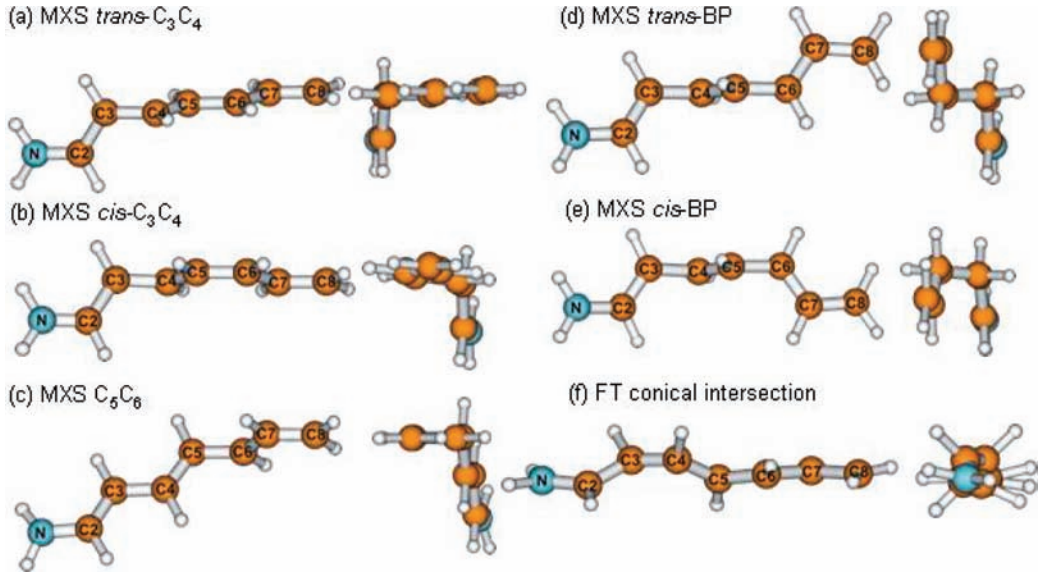

Figure 4. Geometries of the minima on the crossing seam. Each case is shown in two different views.

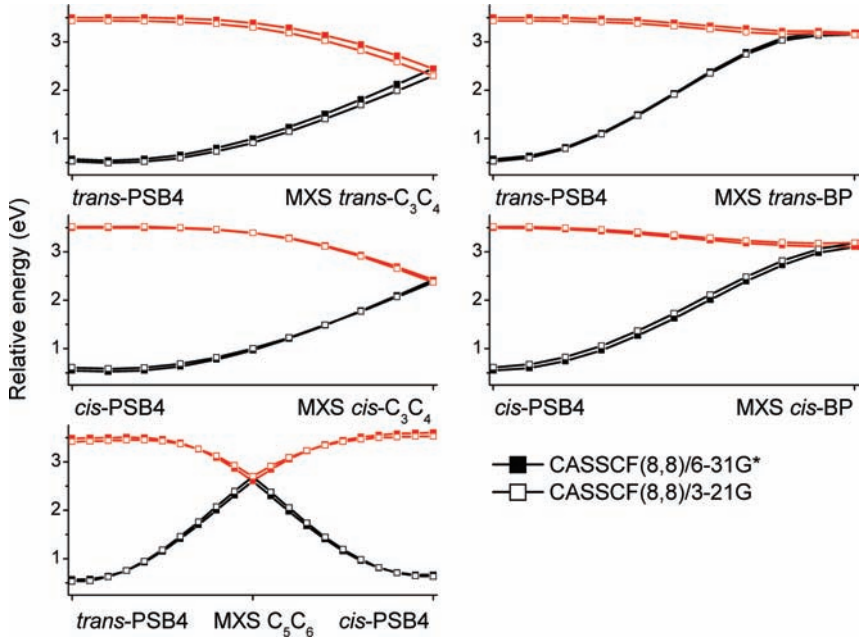

Figure 5. LIIC reaction paths between the planar S_1 minimum of the trans and cis isomers of PSB4 and the MXSs.

very small barrier of 0.02 eV, which certainly will disappear upon relaxation. The paths to the BP MXSs are very flat due to the high energy of the conical intersections (see also Table 2).

Comparison of Theoretical Levels. The choice of the appropriate theoretical level is a very important issue for the efficiency of the dynamics simulations. In the course of the dynamics simulations, several hundred thousands of quantum chemical calculations (energies, gradients, and nonadiabatic coupling vectors) have to be performed. Therefore, a reasonable balance between the quality of the approach (choice of method and basis set) and the computational cost has to be found. Therefore, before starting such time-consuming dynamics simulations, static calculations have been carried out with the aim of assessing the performance of different approaches.

In order to compare the basis set effect on the potential energy surfaces of PSB4, all minima and MXSs discussed in the previous section have been optimized at both the SA-2-CASSCF(8,8)/6-31G* and SA-2-CASSCF(8,8)/3-21G levels. The performance of the 3-21G basis set has been further verified by the LIIC procedure connecting the geometry of the S_1 minimum and the MXSs. Comparison of all these data show that the CASSCF(8,8)/3-21G results agree very well with those obtained with the CASSCF(8,8)/6-31G* method as can be verified by investigation of Table 2 and Figures 3 and 5. The shape of the LIIC paths are very well reproduced by calculations employing the smaller basis set (the relative stabilities of the key points of the photodynamical process are quite similar) independently of the basis sets used. Previous calculations on PSB3 and PSB4[32,40] performing similar validation investigations as the present ones have shown good agreement between CASSCF and MR-CISD results for ground state and S_1 minimum geometries and MXS structures. LIIC paths from the S_1 minimum to the MXSs give similar, very satisfactory accord between different methods. Moreover, vertical excitation energies and the energies of the MXS structures computed at the CASSCF levels agree well with MR-CISD+Q results (Table 2). For further comparison vertical excitation energies computed at the RI-CC2 level are included in Table 2 as well. Also in

TABLE 3: Statistics of the Motions Leading to Conical Intersections (In Percent of Trajectories)

system	OBF		NRBP	BP	FT	no motion/ other motion	no hopping
	C3−C3	C5−C6					
				cis-PSB4			
0 R	11	25	44	14	0	0/3	3
2 R	5	26	41	20	1	0/4	3
4 R	0	0	37	37	15[a]	0/0	11
				trans-PSB4			
0 R	41	3	40	5	0	2/2	7
2 R	27	4	42	0	6	0/3	18
4 R	10	0	29	4	29	1/0	27

[a] Including two trajectories with main torsion around C_5C_6.

this case good match between all data is observed. Similar positive experiences aiming at a cost reduction in the dynamics have been reported recently in several other cases.[40,75,78−80] Combining all just-described experience, the CASSCF(8,8)/3-21G level was chosen for performing dynamic calculations of PSB4.

PSB4 Dynamics. The photodecay of the PSBn systems consists of a two-step process as discussed previously and characterized as a two-state (S_0, and S_1) two-mode (skeletal stretching, and torsional motion around double bond) (TSTM) model.[30,35,81] After photoexcitation, in the initial stage of the dynamics the PSBn system relaxes by adjusting the bonds lengths, elongating the double bonds and shortening the single bonds. This phase, common to all currently studied PSBn systems, has been previously described and will not be analyzed in detail in the present work. After adjusting all bonds, PSBn proceeds to the second step of the dynamics. The crossing seam is reached by skeletal torsions around one or more bonds. When the molecular system switches from the excited state to the ground state it can either continue or reverse its motion that led to the crossing seam and further relax to the final product geometry. All of these aspects related to the torsional stage of the dynamics are the subject of this work.

Mechanisms Leading to the Conical Intersection. Table 3 presents the result of the analysis of the motion leading to the conical intersections for all cases investigated. The first important conclusion that can be drawn from inspection of the table is the importance of the two mechanisms that could not be observed for the PSB3 model,[40] BP and NRBP. The NRBP mode dominates or contributes an important fraction to motions leading to the conical intersection for cis- and trans-PSB4. The BP motion is important for the cis-PSB4 case. The OBF is also of relevance in case of 0 and 2 restrictions. The increasing number of restrictions makes the approach to the intersection seam more difficult for both isomers studied and manifests itself by an increase in the number of trajectories that did not show any hopping at all (from 3 to 11%, and from 7 to 27% for cis and trans isomers, respectively). This is especially important when the dynamics starting at trans-PSB4 with four restricted hydrogen atoms is considered. The sum of the NRBP and BP contributions amounts to 33% with respect to the total number of trajectories. This number increases to 45% when referred to the number of trajectories that hopped to the ground state. It is also worth mentioning that similar to our the previous investigations on PSB3[33,40] none of the trajectories showed the HT mechanism.

When the dynamics starts at cis-PSB4, the most frequent way to reach the seam is through the NRBP mechanism. The amount of trajectories showing this type of motion stays practically constant regardless of given restrictions. On the other hand, a growing number of trajectories presenting BP motion can be observed (14, 20, and 37% for no, two, and four restrictions, respectively). This increase is accompanied by a decreasing amount of OBF motions. For the unrestricted cis-PSB4, the latter group consists mainly (25% of trajectories) of rotations around the C_5C_6 bond (OBF_{56}). The amount of trajectories with OBF around the C_3C_4 bond (OBF_{34}) is by more than a factor 2 smaller (11%) than OBF_{56}. When two restrictions are being applied, this value drops to 5%, while the amount of trajectories showing OBF_{56} is slightly larger (26%). The number of trajectories showing BP motion rises by 6% points, which is the same as the loss in OBF_{34}. These changes suggest that application of two restrictions induces an additional torsion around the C_5C_6 bond. None of the trajectories show the FT mechanism for the unrestricted case and only one percent appears for the doubly restricted system. Application of restrictions to all terminal hydrogens of cis-PSB4 changes the character of the photodecay completely. Isolated single rotations (OBF) are no longer observed and 74% of all trajectories present concerted-twisting mechanisms equally distributed between BP and NRBP. The complete disappearance of OBF comes together with a significant rise of the FT mechanism (15%). Further analysis shows that in the majority (13 out of 15) of FT motions the main torsion is the one around the C_3C_4 bond. The fact combined with the complete disappearance of OBF_{56} implies that for the largest degree of hindrance rotation around the C_3C_4 bond becomes more important than around C_5C_6.

In case of the trans-PSB4 isomer, OBF_{34} and NRBP are the two main and equally contributing mechanisms leading the unrestricted system to the seam (41 and 40%, respectively). Additionally, OBF_{56} and BP mechanisms are observed. Their importance, however, is much smaller (3 and 5%). Similar to the cis isomer and to the previously investigated trans-PSB3, the FT motion is not observed for the unrestricted system. When two restrictions were applied the contribution of OBF_{34} decreases. At the same time the appearance of the FT mechanism is found with a non-negligible contribution of 6%. Still, almost half of the trajectories display the NRBP mechanism which slightly increases its contribution to 42%. The BP motion is not observed. The amount of trajectories showing OBF_{56} decreases from 41 to 27%. When going to the 4-fold restricted system, similarly to the smaller PSB3[40] model, a significant reduction of the contribution from OBF_{34} (from 27 to 10%) is observed accompanied by a large increase (from 6 to 29%) in the amount of trajectories with FT mechanism. This is related to the fact that for the highest degree of hindrance additional adjustments within the chain have to be made in order to allow the molecule to reach the intersection seam. The OBF_{56} mechanism was no longer observed, while BP showed up again (4%). The contribution of NRBP dropped to the level of 29%.

TABLE 4: Motions after the Hopping [In Percent of Trajectories at the Time of Hopping (See Table 3)][a]

	OBF												FT				
	C_3C_4		C_5C_6		NRBP				BP				C_3C_4		C_5C_6		
system	C	R	C	R	C	P(C_3C_4)	P(C_5C_6)	R	C	P(C_3C_4)	P(C_5C_6)	R	C	R	C	R	no. classif possible[b]
									cis-PSB4								
0 R	82	18	44	44	16	25	27	23	29	50	7	14					7
2 R	40	40	69	23	24	24	22	15	10	50	10	15	100	0	0	0	12
4 R					27	38	0	19	14	43	0	30	67	20	50	50	11
									trans-PSB4								
0 R	61	22	100	0	3	48	8	23	40	60	0	0					15
2 R	63	33	50	50	2	50	10	26					83	17	0	0	6
4 R	50	50			7	17	0	41	0	25	0	50	62	31	0	0	13

[a] Abbreviations: C, continued; R, reversed; P(*X*), partially continued, X is the torsional axis. [b] Relative to all trajectories assigned to the given (OBF, FT, NRBP, BP) types.

Additionally, it should be noted that more than one-quarter of trajectories did not hop to the ground state.

In summary, the analysis of the mechanisms leading trans-PSB4 to the seam of conical intersections implies the coexistence of two groups of mechanisms. The first group includes OBF and FT mechanisms and proceeds such as to produce a complete torsion around only one bond, mostly around C_3C_4. The second group, which includes BP and NRBP, produces concerted twists around two bonds, C_3C_4 and the C_5C_6. With the variation in the degree of restriction, the transfer from one mechanism to the other tends to occur within the same group. The overall contributions from both groups stay at approximately the same level, both representing around half of trajectories reaching the seam. Different conclusions, however, can be drawn for the dynamics starting at the cis-PSB4 isomer. Here, a dominating character of the double-torsion group of mechanisms can be observed, which is about twice as frequent as the single-torsion group up to two restrictions and rises to almost five times when four restrictions are applied. Generally, the importance of torsion around C_5C_6 is larger for the dynamics starting at the cis isomer than at the trans isomer. On the other hand, when restrictions are applied to all terminal hydrogens the rotation around C_3C_4 becomes the most abundant motion in both cases.

Assignment of the FT motion to the first group of mechanisms, although consisting of three concerned torsions, is mainly related to the nature of the entire FT process. Similar to findings for PSB3,[40] in all PSB4 trajectories undergoing FT mechanism only the main torsion was continued after hopping to the ground state with immediate reversion of two accompanying torsional motions. Thus FT can be understood as a way of performing an OBF twist in highly strained systems. On the other hand, NRBP is assigned to the group of double torsion restrictions because in this mechanism the second torsion is not only an auxiliary way to perform the main torsion, but it tends to continue itself after hopping. (The reversion and continuation of the mechanisms will be discussed in detail in the next section.)

Motions after Surface Hopping. When returning to the ground state, the excess of electronic energy is converted into mechanical energy. In this vibrationally hot ground state, there will be freedom to move into different conformations, which are usually confined by high potential energy barriers. The transfer of the mechanical energy to the protein will take at least several picoseconds,[24] which means that the motion in the hot ground state may be decisive for the quantum yields. In this section, the question of the hot ground-state motion is addressed from two points of view. First, we investigate whether the mechanism bringing PSB4 to the intersection seam is reversed or not after hopping. Second, the question is investigated whether the initial motion results in the associated product or not.

As discussed in the previous sections, the mechanisms driving the molecular system to the crossing seam can be assigned to two groups, the single-torsion group, which includes the OBF and the FT mechanisms, and the double-torsion group, which includes the BP and the NRBP mechanisms. This distinction will be useful in the discussion of how the motion is continued in the ground state. More specifically, in the ground state the preceding motion leading to the conical intersection can be continued (denoted as "C" in Table 4), reversed (denoted as "R"), or undetermined. The latter case applies to a situation where PSB4 stays in the vicinity of the conical intersection, at least for the time of analysis. In the case of mechanisms featuring double torsions (NRBP, BP) there is one additional possibility: the motion can be partially continued, that is, the torsion around one of the bonds proceeds while the other one reverses (noted as "P(X)", where X is the bond around which the torsion proceeds). We define as an associated product an isomer that is formed by a continuation of a specific motion in the ground state. For example, if the trans-PSB4 undergoes an OBF_{34} and continues the motion after hopping, it will end up in the 3-cis-PSB4 associated product. The cis-PSB4 moving to the seam by means of OBF_{56} has as associated product the all-trans-PSB4 isomer. This concept will be useful to determine the final products of the dynamics.

Single-Torsion Group of Mechanisms (OBF, FT). The analysis is started with the cis-PSB4 isomer (see Table 4). In case of unrestricted OBF_{34} the majority (82%) of trajectories consist of continued torsion that led the system to the conical intersection. On the other hand, for OBF_{56} there are equal fractions (44%) of trajectories with continued or reversed motion after hopping. When two restrictions were applied to cis-PSB4, the rate of continued OBF_{34} drops to 40% while for OBF_{56} the ratio of continued motion rises to 69%. As was discussed in the previous section, for four restrictions OBF is no longer observed and the ratio of continued FT motions assumes a level of 67%.

Further analysis concerning the question whether the examined motion leads to the associated product or not within 60 fs after hopping is presented in Table 5. It shows that for both cases of single-torsion motions (OBF and FT) in cis-PSB4 the continued motion resulted entirely in formation of the OBF associated product. In particular, it is noted that in all occurrences of the FT mechanism the two *partial* torsions were always reversed after hopping. These *partial* torsions give

TABLE 5: Fraction of Trajectories (In Percent of Continued Motion Given in Table 4) Leading to the Associated Product after Hopping (See Text for Explanation)[a]

	OBF		NRBP			BP			
	cont motion		cont motion			cont motion			FT
system	C_3C_4	C_5C_6	C_3C_4 and C_5C_6	C_3C_4	C_5C_6	C_3C_4 and C_5C_6	C_3C_4	C_5C_6	cont motion
					cis-PSB4				
0R	100	100	0 (71)	73	100	75 (25)	86	100	
2R	100	100	20 (80)	90	100	50 (0)	90	100	100
4R			0 (50)	57	0	40 (40)	94	0	100
					trans-PSB4				
0R	88	100	0 (0)	100	100	100 (0)	100	0	
2R	100	100	0 (100)	100	100				100
4R	80		0 (100)	60	0	0 0	100	0	100

[a] In parentheses, percentages of trajectories resulting in product formation corresponding to OBF_{34} or OBF_{56} are given (assigned to fully continued BP or NRBP motion).

TABLE 6: Summary of Photoproduct Analysis (In Percent of All Trajectories) after the Hopping (Given in Table 5) and at the End of the Dynamics (Values in Parentheses)

	cis-PSB4 ($\varepsilon\varepsilon\varepsilon\varepsilon\zeta\varepsilon\varepsilon$)				*trans*-PSB4 ($\varepsilon\varepsilon\varepsilon\varepsilon\varepsilon\varepsilon\varepsilon$)			
corresponding motion	product	0R	2R	4R	product	0R	2R	4R
	$\varepsilon\varepsilon\varepsilon\varepsilon\zeta\varepsilon\varepsilon$	25(17)	27(20)	37(22)	$\varepsilon\varepsilon\varepsilon\varepsilon\varepsilon\varepsilon\varepsilon$	21(7)	24(19)	27(24)
OBF_{34}	$\varepsilon\varepsilon\zeta\varepsilon\zeta\varepsilon\varepsilon$	22(11)	22(22)	27(31)	$\varepsilon\varepsilon\zeta\varepsilon\varepsilon\varepsilon\varepsilon$	41(27)	45(40)	35(8)
OBF_{56}	$\varepsilon\varepsilon\varepsilon\varepsilon\varepsilon\varepsilon\varepsilon$	34(17)	19(12)		$\varepsilon\varepsilon\varepsilon\varepsilon\zeta\varepsilon\varepsilon$	2(2)	3(3)	
BP	$\varepsilon\varepsilon\zeta\varepsilon\varepsilon\varepsilon\varepsilon$	3(3)	3(1)	3(2)	$\varepsilon\varepsilon\zeta\varepsilon\zeta\varepsilon\varepsilon$	1(1)		
other		(5)				1(7)		(8)[a]
not assigned		12(43)	19(35)	27(39)		11(33)	8(18)	13(35)
no hopping[b]		4(4)	10(10)	6(6)		23(23)	20(20)	25(25)

[a] $\varepsilon\varepsilon\zeta\varepsilon\varepsilon\zeta\varepsilon$. [b] Excluded from analysis.

sufficient flexibility to the restricted system to perform the full torsion around only one main bond.

In the case of the trans-PSB4 isomer, the effect of the degree of restriction is more directly correlated to the ratios of motions classified as continued or reversed. As discussed in the previous section, the single-torsion events are here almost entirely connected to rotation around C_3C_4. Table 4 shows that for the torsion around this bond the amount of reversed motions systematically increases as a function of the degree of restriction (22, 33, and 50% for no, two, and four restrictions). The same trend is observed in the FT and in the OBF_{56} mechanisms.

Table 5 shows that the majority of OBF_{34} continued motions lead to the associated product, the 3-cis-PSB4 isomer. Nevertheless, it is worth noting that for the unrestricted and 4-fold restricted trans-PSB4 12 and 20%, respectively, of the cases the motion turned back to the all-trans structure without even temporarily forming 3-cis-PSB4.

Double-Torsion Group of Mechanisms (BP, NRBP). The analogous analysis of the two-torsion mechanism results in a more complicated picture than was found for the single-torsion case. Now, the system cannot only continue or reverse both torsions, but also partially continue them, that is, continue one torsion while reversing the other. The results presented in Table 4 show significantly larger rates for complete continuation of the NRBP motion for cis-PSB4 than for the trans isomer. Interestingly, despite the large fraction of continued NRBP motion (16, 24, and 27% for no, two, and four restrictions, respectively) in the majority of cases (see Table 5) this fact does not result in formation of the associated product, that is, the 3-cis-PSB4. For all-trans-PSB4, we do not observe any case where continued NRBP motion leads to formation of the associated 3,5-cis-PSB4, even not temporarily. On the other hand, when the motion leading to the conical intersection is reversed after hopping, reversion proceeds completely in almost all cases regardless of the type of motion and system. The largest difference between NRBP and BP is related to the formation of the associated photoproduct for the continued BP motion fractions of formation are 75, 50, and 40% (for no, two, and four restrictions respectively) for the cis isomer.

The most abundant way of continuation of concerted double-torsion motions is not a complete continuation or reversion, but partial continuation. The results in Table 4 show that for unrestricted cis-PSB4 the torsion around the C_5C_6 bond is continued slightly more frequently than the one around the C_3C_4 bond (27 and 25% for NRBP). Nevertheless, when restrictions are imposed, the relative proportions gradually changes, increasing for torsion around C_3C_4 and decreasing for C_5C_6 (24 vs 22% and 38 vs 0% for systems with two and four restrictions). For the all-trans isomer rates of partial continuation of the rotation around the C_3C_4 bond are significantly higher (over 5 times) than rotations around C_5C_6, which similarly to cis-PSB4 are not present for the highly restricted system. The majority of partially continued torsions around C_3C_4 results in the associated product formation. Interestingly, when partial continuation around C_5C_6 is considered it proceeds completely in all cases regardless of the type of motion and isomer.

Final Products. As last step of the structural analysis, the final product at the end of the dynamics was determined (see Table 6). This assignment was performed independently of the mechanistic analysis presented above by investigating the structure at the last step of each trajectory. It is interesting to note that the differences between the yields of product formation examined after the hopping to the ground state and at the end of the dynamics are substantial, especially for the unrestricted case. They reflect the changes due to the vibrationally hot dynamics in the ground state after the initial product assignment was made. This is also manifested by the large number of structures that could not be assigned to one of the types of

TABLE 7: Parameters for Fitting Average S_1 Occupation and Resulting S_1 Lifetimes (See Text for Explanation)

system	restrictions	t_d (fs)	t_e (fs)	τ (fs)
cis-PSB4	0	68	46	114
	2	70	60	130
	4	72	67	139
trans-PSB4	0	74	65	139
	2	69	73	142
	4	71	96	167

torsional motion at the end of the dynamics since at least one of the dihedral angles was located between 60 and 120°, that is, far away from planarity. Because of the large number of undetermined motions it is difficult to distinguish trends in the product formation. However, in both cases of doubly restricted cis- and trans-PSB4 systems, which model rhodopsin and bacteriotrhodopsin chromophore, respectively, exceptionally large amounts (see Table 6) of product formation are observed.

Lifetimes. Average S_1 occupations, defined as the fraction of trajectories in the excited state, were computed in order to estimate the lifetimes. Similar to previous studies,[16,21,24,33,40,41,43,75] the S_1 occupation remains constant for a short initial time period t_d after which it starts to decay exponentially with time constant t_e. The lifetimes $\tau = t_d + t_e$ were obtained by fitting the S_1-state occupation with the function $f(t) = \exp(-(t - t_d)/t_e)$ for all systems studied. The fitting parameters and the lifetimes are given in Table 7. For both isomers of PSB4, a systematic increase of the lifetimes (114, 130, and 139 fs, and 139, 142, and 167 fs for no, two, and four restrictions for cis and trans isomers, respectively) is observed, which is consistent with the increasing number of restrictions making it increasingly difficult to reach the conical intersection. For the cis isomer, the increase in lifetime from no to two and from to two to four restrictions are of similar magnitude. A different situation is found for the trans isomer. The change from no to two restrictions has a rather small influence on the lifetime whereas the change from two to four restrictions is more significant. A similar behavior has been previously obtained for the smaller PSB3 model[40] although the currently obtained lifetimes for trans-PSB4 are systematically longer by 30−40 fs in comparison to the similarly restricted trans-PSB3.[40] The lifetimes obtained in the course of the present work fit well into the range of previous theoretical (80−200 fs)[15,20,23,27,29,43] and experimental (100−500 fs)[10,12,13,82,83] findings on Rh and bR and their models. The comparison with experimental data, however, should be performed with care because of the need to use even larger PSB chains and because of different environmental conditions. For instance, a much slower isomerization dynamics of retinal protonated Schiff bases was reported for several different solvents.[84]

Implications for Rhodopsin and Bacteriorhodopsin. The isomerization mechanisms of cis- and trans-PSB4 in the excited and ground states has been investigated by systematically changing the degree of mechanical restrictions applied to the molecule. In this section, we focus on the doubly restricted PSB4 (2r-PSB4) for which the cis and trans isomers are assumed to be our best models for rhodopsin (Rh) and bacteriorhodopsin (bR), respectively. In summary, the dynamics of both trans- and cis-2r-PSB4 can be described in the following way (see Figure 6). After the photoexcitation, 2r-PSB4 quickly relaxes to a region of strongly distorted geometries, where the internal conversion can occur. The time to reach this region is about $t_d = 70$ fs (Table 7). The internal conversion occurs 60 fs later for cis-2r-PSB4 and 73 fs later for trans-2r-PSB4, which means that the internal conversion occurs in average 130 fs (cis) or 142 fs (trans) after the photoexcitation. The NRBP mechanism is the

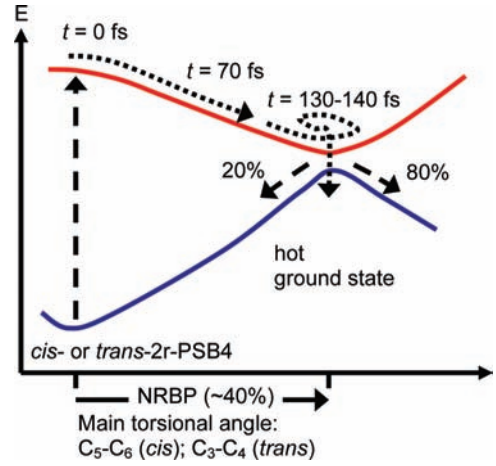

Figure 6. Scheme of the dynamics of the doubly restricted PSB4 starting at the cis and trans isomers as obtained from the simulations.

most important mechanism driving 2r-PSB4 isomerization in the excited state (Table 3). BP and OBF around C_5C_6 are also relevant for the cis isomer, while OBF around C_3C_4 is relevant for the trans isomer. In any case, the OBF is facilitated by accompanied torsions of less than 30°. About 20% of trajectories return to the initial isomer in the ground state (Table 6). Most of the other trajectories form several different kinds of vibrationally hot structures at the end of the simulations (200 fs) without clear decision about the final isomer that will be obtained after cooling down by the interaction with the environment. In the remaining part of this section, comparison to experimental findings for Rh and bR[1,4,10,13,82,85−87] are made with the goal to establish on the one hand the usefulness of the doubly restricted PSB4 model and on the other hand to shed light on the isomerization mechanisms occurring in Rh and bR.

In the last two decades, a large effort of the theoretical modeling of the Rh and bR photobehavior has focused on the single-torsion motion as the main isomerization mechanism. These predictions however were based mostly on calculations of the minimum energy path or dynamics on the shorter PSB3 model.[35,36,40−43] On the other hand, investigations on longer PSB chains in earlier works by Warshel[27,28] or in more recent investigations[15,17,20,23,26] indicate that double-torsion mechanisms like BP or NRBP should be the main isomerization mechanisms. Also the present results, based on statistical material derived from extensive ab initio dynamics simulations strongly indicate that RPSB isomerizes in the excited state by performing two concerted twist motions from which only one tends to be continued during the relaxation into the ground state. The main isomerization trend is a torsion around C_5C_6 (equivalent to $C_{11}C_{12}$ in RPSB) in the case of the cis isomer and around C_3C_4 ($C_{13}C_{14}$ in RPSB) in the case of the trans isomer. Torsional motions of similar character were observed in the recent works by Buss and co-workers,[15,16] who also investigated PSB4 augmented by two additional methyl groups in the C_4 and C_8 positions. Interestingly, for the rhodopsin model (cis-PSB4) the results of Warshel[27,28] and the recent QM/MM dynamic studies on the complete RPSB[17] point to BP and NRBP motions around C_5C_6/C_7C_8 instead of C_3C_4/C_5C_6. This difference could suggest that either the chain length in 2r-cis-PSB4 is still too short or that the methyl group in C_{13} of RPSB is important. On the other hand, trans-PSB4 as a model of bR is not affected by these limitations, since the main isomerization occurs in the C_3C_4 bond, thus the system size is suitable for performing double-torsion isomerization. It is also worth mentioning that QM/MM

simulations of full RPSB employing the restricted open-shell Kohn−Sham (ROKS) method[49] do not support double-torsions mechanism, pointing entirely to OBF as a way of performing photoisomerization in the Rh pocket. At the same time QM/MM minimum energy path investigations of the same system[50] report non-negligible involvement of four additional torsions to the main torsion in the isomerization process.

The lifetime of the photoisomerization process of rhodopsin and bactriorhodopsin chromophore is a widely discussed issue. The uncertainties are mostly related to the fact that the structures of intermediates are still unknown. Although our theoretical model in gas phase cannot be directly compared to the experimental results obtained in the protein environment, the dynamics results bring qualitative information that can shed light on this question. Femtosecond transient absorption spectroscopic studies by the group of Mathies[53] indicate that rhodopsin leaves the Franck−Condon region toward a region of the potential energy surface weakly dipole-coupled to the ground state in about 50 fs. Later on, this highly distorted isomer switches to the ground state in ∼200 fs to form the first ground state photoproduct.[4,54] Our simulations showing an initial 70 fs relaxation into twisted regions corresponding to the aforementioned weakly dipole-coupled region with the ground state and giving an average internal conversion time of 130−140 fs are fully compatible with this experimental scenario. More recently, based on femtosecond-stimulated Raman spectroscopy, a different interpretation for these two time constants has been proposed,[10] attributing the 50 fs constant to the time for internal conversion to the ground state and the 200 fs time constant to the time to form the photoproduct in the ground state. According to this interpretation, the internal conversion would occur at conical intersections with a small degree of torsion compensated by strong hydrogen out-of-plane distortions. This second interpretation is not compatible with the results of our simulations, which clearly demonstrate the importance of the torsional modes. In the case of bacteriorhodopsin, experimental studies[13,82] indicate that the internal conversion takes place in ∼500 fs, which is much longer as compared to our computed time of 140 fs. This difference could indicate that the restrictions imposed by the protein pocket are stronger for bR, retarding the isomerization process.

Conclusions

In this work the results of ab initio surface-hopping dynamics simulations for the all-trans- and 5-cis-hepta-3,5,7-trieniminium cation (trans- and cis-PSB4) are presented for unrestricted and restricted dynamics using two sets of mechanical restrictions in the latter case. In the first set, two terminal hydrogen atoms on opposite ends of the PSB4 chain were fixed by increasing their masses. In the second set, all four terminal hydrogen atoms were restricted. Our main goal has been to analyze the actual mechanism occurring in the dynamics of PSB4 in view of the different idealized mechanisms (OBF, BP, NRBP, HT, and FT). Extended samples of 600 trajectories were computed.

At the beginning, a survey of important sections of the ground- and excited-state energy surfaces for cis- and trans-PSB4 including the determination of five minima on the seam of conical intersections has been performed. Methodological comparisons at MRCI and CASSCF levels using different basis sets were carried out in order to find the best-suited quantum chemical method in terms of quality and computational cost for the dynamics simulations.

The statistical analysis shows that for the first stage of the dynamics (the motion leading to the conical intersection) in all investigated cases the nonrigid bipedal (NRBP) is the main mechanism. Its importance does not vary much with the number of imposed restrictions, ranging between 37−44% and 29−42% for cis and trans isomer, respectively. The occurrence of the BP mechanism, however, varies with the isomers. Its importance increases with the number of restricted atoms for the cis isomer and stays on a very low level for the trans isomer. The FT mechanism, which has been identified recently in the dynamics of PSB3,[40] was also observed to occur in PSB4 with two and four restrictions. Although the FT is statistically not important for the unrestricted and doubly restricted case, it is one of the two main mechanisms when the four restrictions are applied to trans-PSB4. It has also been identified as the only way to perform single torsion isomerization of cis-PSB4 with four restrictions. Additionally, no case of photodecay featuring HT has been observed during simulations, regardless of the isomer or degree of restriction imposed.

The general picture obtained from analysis of PSB4 differs significantly from the one observed for PSB3. For the latter model, no other standard mechanism besides the OBF and the FT has been observed, even when four restrictions were imposed. The analysis of the motions of both isomers of PSB4 shows, however, that the double-torsion mechanisms (NRBP and BP) are the main ways for reaching the conical intersection seam. Their contributions are exceptionally high for the cis-PSB4, but also for all-trans isomer they constitute around half of the motions leading to the seam.

The analysis of the second stage of the dynamics, the motion after hopping to the ground state, completes the picture of the dynamics. Here significant reversion of trends to perform double-torsion motions (BP and NRBP) can be seen. Most of the trajectories showing NRBP or BP continue the torsional motion in only one of the bonds, reversing the torsion in the other one. But even when there is continuation of torsion around both bonds, this does not necessarily result in the formation of the associated product. Moreover, analysis of the PSB4 behavior after leaving the neighborhood of the conical intersection shows the presence of additional motions that may appear induced by the hot ground-state dynamics. This is illustrated by a large number of unassignable structures at the end of simulation and the differences between product fractions derived from direct continuation of the motion leading to the conical intersection and the actual distribution of corresponding structures at the end of simulation.

For PSB4 with two restrictions, considered as our best model for RPSB embedded in rhodopsin, it is found that the NRBP motion is one main mechanism responsible for the photoisomerization process. It occurs by means of a partial torsion around one bond functioning as auxiliary mode for delivering the full torsion around a second bond. Thus, the main isomerization is a torsion around C_5C_6 (equivalent to $C_{12}C_{11}$ in RPSB) in the case of the cis isomer and around C_3C_4 ($C_{14}C_{13}$ in RPSB) in the case of the trans isomer. The isomerization mechanism brings the molecule to twisted configurations in about 70 fs and the internal conversion occurs in about 140 fs. After the conversion, the molecule returns to the hot ground state forming the initial isomer in about 20% and different products in the remaining 80% of the cases.

The dynamics of PSB4 can be considered a qualitative advance in comparison to the PSB3 case for revealing the role of multiple-bond torsional mechanisms. The next natural step in this sequence of models of Rh and bR chromophores investigations is to perform a full nonadiabatic dynamics for RPSB. Although we argued that all-trans-PSB4 is already a

suitable model for RPSB behavior in bR, it is expected that in the case of Rh model inclusion of at least one more double bond affects the distribution of mechanisms relative to PSB4 or even reveals new mechanisms. In any case, the classification algorithms presented here are general enough to tackle its analysis. In the present investigation, environmental influences were reduced to the mechanical restrictions imposed by the protein and the remaining RPSB molecule. This limits the degree to which our results can be compared to experimental data, usually measured in the protein environment or in solution. Although we are confident that explanations have been presented that should be valid at a qualitative level even for more complex systems, further investigations are required considering also electronic effects induced by the protein environment or by solution including a counterion. Work along these lines is in progress in our group.

Acknowledgment. The authors also acknowledge the technical support and computer time at the Linux PC cluster Schrödinger III of the computer center of the University of Vienna, Poznan Supercomputing and Networking Centre, and Wroclaw Centre for Networking and Supercomputing at Wroclaw University of Technology. This work was supported by the Austrian Science Fund within the framework of the Special Research Program F16 (Advanced Light Sources) and Project P18411-N19. Support by the grant from the Ministry of Education of the Czech Republic (Center for Biomolecules and Complex Molecular Systems, LC512) and by the Praemium Academiae of the Academy of Sciences of the Czech Republic, awarded to Pavel Hobza in 2007, is gratefully acknowledged. This work was part of the research project Z40550506 of the Institute of Organic Chemistry and Biochemistry of the Academy of Sciences of the Czech Republic.

Supporting Information Available: Cartesian geometries for all structures discussed in Table 2. This material is available free of charge via the Internet at http://pubs.acs.org.

References and Notes

(1) Birge, R. R. *Biochim. Biophys. Acta* **1990**, *1016*, 293.
(2) Palings, I.; Pardoen, J. A.; Vandenberg, E.; Winkel, C.; Lugtenburg, J.; Mathies, R. A. *Biochemistry* **1987**, *26*, 2544.
(3) Birge, R. R. *Annu. Rev. Biophys. Bioeng.* **1981**, *10*, 315.
(4) Schoenlein, R. W.; Peteanu, L. A.; Mathies, R. A.; Shank, C. V. *Science* **1991**, *254*, 412.
(5) Wang, Q.; Schoenlein, R. W.; Peteanu, L. A.; Mathies, R. A.; Shank, C. V. *Science* **1994**, *266*, 422.
(6) Neutze, R.; Pebay-Peyroula, E.; Edman, K.; Royant, A.; Navarro, J.; Landau, E. M. *Biochim. Biophys. Acta, Biomembr.* **2002**, *1565*, 144.
(7) Haupts, U.; Tittor, J.; Oesterhelt, D. *Annu. Rev. Biophys. Biomol. Struct.* **1999**, *28*, 367.
(8) Oesterhelt, D.; Tittor, J.; Bamberg, E.; Haupts, U. *FASEB J.* **1997**, *11*, A992.
(9) Wald, G. *Science* **1968**, *162*, 230.
(10) Kukura, P.; McCamant, D. W.; Yoon, S.; Wandschneider, D. B.; Mathies, R. A. *Science* **2005**, *310*, 1006.
(11) Schenkl, S.; van Mourik, F.; Friedman, N.; Sheves, M.; Schlesinger, R.; Haacke, S.; Chergui, M. *Proc. Natl. Acad. Sci. U.S.A.* **2006**, *103*, 4101.
(12) Kobayashi, T.; Saito, T.; Ohtani, H. *Nature* **2001**, *414*, 531.
(13) McCamant, D. W.; Kukura, P.; Mathies, R. A. *J. Phys. Chem. B* **2005**, *109*, 10449.
(14) Garavelli, M.; Negri, F.; Olivucci, M. *J. Am. Chem. Soc.* **1999**, *121*, 1023.
(15) Schapiro, I.; Weingart, O.; Buss, V. *J. Am. Chem. Soc.* **2009**, *131*, 16.
(16) Weingart, O.; Schapiro, I.; Buss, V. *J. Phys. Chem. B* **2007**, *111*, 3782.
(17) Hayashi, S.; Taikhorshid, E.; Schulten, K. *Biophys. J.* **2009**, *96*, 403.
(18) Send, R.; Sundholm, D. *J. Phys. Chem. A* **2007**, *111*, 8766.
(19) Ben-Nun, M.; Molnar, F.; Lu, H.; Phillips, J. C.; Martinez, T. J.; Schulten, K. *Faraday Discuss.* **1998**, 447.
(20) Frutos, L. M.; Andruniow, T.; Santoro, F.; Ferre, N.; Olivucci, M. *Proc. Natl. Acad. Sci. U.S.A.* **2007**, *104*, 7764.
(21) Hayashi, S.; Tajkhorshid, E.; Schulten, K. *Biophys. J.* **2003**, *85*, 1440.
(22) Rohrig, U. F.; Guidoni, L.; Rothlisberger, U. *ChemPhysChem* **2005**, *6*, 1836.
(23) Saam, J.; Tajkhorshid, E.; Hayashi, S.; Schulten, K. *Biophys. J.* **2002**, *83*, 3097.
(24) Birge, R. R.; Hubbard, L. M. *Biophys. J.* **1981**, *34*, 517.
(25) Logunov, I.; Schulten, K. *J. Am. Chem. Soc.* **1996**, *118*, 9727.
(26) Andruniow, T.; Ferre, N.; Olivucci, M. *Proc. Natl. Acad. Sci. U.S.A.* **2004**, *101*, 17908.
(27) Warshel, A. *Nature* **1976**, *260*, 679.
(28) Warshel, A.; Barboy, N. *J. Am. Chem. Soc.* **1982**, *104*, 1469.
(29) Warshel, A.; Chu, Z. T. *J. Phys. Chem. B* **2001**, *105*, 9857.
(30) González-Luque, R.; Garavelli, M.; Bernardi, F.; Merchán, M.; Robb, M. A.; Olivucci, M. *Proc. Natl. Acad. Sci. U.S.A.* **2000**, *97*, 9379.
(31) Wanko, M.; Hoffmann, M.; Strodel, P.; Koslowski, A.; Thiel, W.; Neese, F.; Frauenheim, T.; Elstner, M. *J. Phys. Chem. B* **2005**, *109*, 3606.
(32) Aquino, A. J. A.; Barbatti, M.; Lischka, H. *ChemPhysChem* **2006**, *7*, 2089.
(33) Barbatti, M.; Ruckenbauer, M.; Szymczak, J. J.; Aquino, A. J. A.; Lischka, H. *Phys. Chem. Chem. Phys.* **2008**, *10*, 482.
(34) Garavelli, M.; Bernardi, F.; Robb, M. A.; Olivucci, M. *J. Mol. Struct.* **1999**, *463*, 59.
(35) Garavelli, M.; Celani, P.; Bernardi, F.; Robb, M. A.; Olivucci, M. *J. Am. Chem. Soc.* **1997**, *119*, 6891.
(36) Migani, A.; Robb, M. A.; Olivucci, M. *J. Am. Chem. Soc.* **2003**, *125*, 2804.
(37) Ruiz, D. S.; Cembran, A.; Garavelli, M.; Olivucci, M.; Fuss, W. *Photochem. Photobiol.* **2002**, *76*, 622.
(38) Sinicropi, A.; Migani, A.; De Vico, L.; Olivucci, M. *Photochem. Photobiol. Sci.* **2003**, *2*, 1250.
(39) Sumita, M.; Saito, K. *Chem. Phys. Lett.* **2006**, *424*, 374.
(40) Szymczak, J. J.; Barbatti, M.; Lischka, H. *J. Chem. Theory Comput.* **2008**, *4*, 1189.
(41) Vreven, T.; Bernardi, F.; Garavelli, M.; Olivucci, M.; Robb, M. A.; Schlegel, H. B. *J. Am. Chem. Soc.* **1997**, *119*, 12687.
(42) Weingart, O.; Migani, A.; Olivucci, M.; Robb, M. A.; Buss, V.; Hunt, P. *J. Phys. Chem. A* **2004**, *108*, 4685.
(43) Weingart, O.; Schapiro, I.; Buss, V. *J. Mol. Model.* **2006**, *12*, 713.
(44) Wanko, M.; Hoffmann, M.; Strodet, P.; Koslowski, A.; Thiel, W.; Neese, F.; Frauenheim, T.; Elstner, M. *J. Phys. Chem. B* **2005**, *109*, 3606.
(45) Cembran, A.; Bernardi, F.; Olivucci, M.; Garavelli, M. *J. Am. Chem. Soc.* **2004**, *126*, 16018.
(46) Migani, A.; Olivucci, M. *Conical Intersections: Electronic Structure, Dynamics & Spectroscopy*; World Scientific Publishing Company: River Edge, NJ, 2004.
(47) Tomasello, G.; Olaso-Gonzalez, G.; Altoe, P.; Stenta, M.; Serrano-Andres, L.; Merchan, M.; Orlandi, G.; Bottoni, A.; Garavelli, M. *J. Am. Chem. Soc.* **2009**, *131*, 5172.
(48) Burghardt, I.; Cederbaum, L. S.; Hynes, J. T. *Faraday Discuss.* **2004**, *127*, 395.
(49) Rohrig, U. F.; Guidoni, L.; Laio, A.; Frank, I.; Rothlisberger, U. *J. Am. Chem. Soc.* **2004**, *126*, 15328.
(50) Gascon, J. A.; Batista, V. S. *Biophys. J.* **2004**, *87*, 2931.
(51) Warshel, A.; Karplus, M. *J. Am. Chem. Soc.* **1972**, *94*, 5612.
(52) Liu, R. S. H.; Asato, A. E. *Proc. Natl. Acad. Sci. U.S.A.* **1985**, *82*, 259.
(53) Kochendoerfer, G. G.; Mathies, R. A. *J. Phys. Chem.* **1996**, *100*, 14526.
(54) Peteanu, L. A.; Schoenlein, R. W.; Wang, Q.; Mathies, R. A.; Shank, C. V *Proc. Natl. Acad. Sci. U.S.A.* **1993**, *90*, 11762.
(55) Tully, J. C. *J. Chem. Phys.* **1990**, *93*, 1061.
(56) Tully, J. C. *Faraday Discuss.* **1998**, *110*, 407.
(57) Bunge, A. *J. Chem. Phys.* **1970**, *53*, 20.
(58) Shepard, R. The Analytic Gradient Method for Configuration Interaction Wave Functions. In *Modern Electronic Structure Theory*; Yarkony, D. R., Ed.; World Scientific: Singapore, 1995; Vol. 1; p 345.
(59) Langhoff, S. R.; Davidson, E. R. *Int. J. Quantum Chem.* **1974**, *8*, 61.
(60) Bruna, P. J.; Peyerimhoff, S. D.; Buenker, R. J. *Chem. Phys. Lett.* **1980**, *72*, 278.
(61) Hehre, W. J.; Ditchfield, R.; Pople, J. A. *J. Chem. Phys.* **1972**, *56*, 2257.
(62) Binkley, J. S.; Pople, J. A.; Hehre, W. J. *J. Am. Chem. Soc.* **1980**, *102*, 939.
(63) Swope, W. C.; Andersen, H. C.; Berens, P. H.; Wilson, K. R. *J. Chem. Phys.* **1982**, *76*, 637.
(64) Butcher, J. *J. Assoc. Comput. Mach.* **1965**, *12*, 124.
(65) Granucci, G.; Persico, M. *J. Chem. Phys.* **2007**, *126*, 134114.
(66) Hammes-Schiffer, S.; Tully, J. C. *J. Chem. Phys.* **1994**, *101*, 4657.

(67) Barbatti, M.; Lischka, H. *J. Phys. Chem. A* **2007**, *111*, 2852.

(68) Lischka, H.; Shepard, R.; Brown, F. B.; Shavitt, I. *Int. J. Quantum Chem.* **1981**, *S.15*, 91.

(69) Lischka, H.; Shepard, R.; Pitzer, R. M.; Shavitt, I.; Dallos, M.; Müller, T.; Szalay, P. G.; Seth, M.; Kedziora, G. S.; Yabushita, S.; Zhang, Z. Y. *Phys. Chem. Chem. Phys.* **2001**, *3*, 664.

(70) Lischka, H.; Shepard, R.; Shavitt, I.; Pitzer, R. M.; Dallos, M.; Müller, T.; Szalay, P. G.; Brown, F. B.; Ahlrichs, R.; Boehm, H. J.; Chang, A.; Comeau, D. C.; Gdanitz, R.; Dachsel, H.; Ehrhardt, C.; Ernzerhof, M.; Höchtl, P.; Irle, S.; Kedziora, G.; Kovar, T.; Parasuk, V.; Pepper, M. J. M.; Scharf, P.; Schiffer, H.; Schindler, M.; Schüler, M.; Seth, M.; Stahlberg, E. A.; Zhao, J.-G.; Yabushita, S.; Zhang, Z.; Barbatti, M.; Matsika, S.; Schuurmann, M.; Yarkony, D. R.; Brozell, S. R.; Beck, E. V.; Blaudeau, J.-P. *COLUMBUS, an ab initio electronic structure program*, release 5.9.1, 2006, www.univie.ac.at/columbus.

(71) Shepard, R.; Lischka, H.; Szalay, P. G.; Kovar, T.; Ernzerhof, M. *J. Chem. Phys.* **1992**, *96*, 2085.

(72) Lischka, H.; Dallos, M.; Shepard, R. *Mol. Phys.* **2002**, *100*, 1647.

(73) Lischka, H.; Dallos, M.; Szalay, P. G.; Yarkony, D. R.; Shepard, R. *J. Chem. Phys.* **2004**, *120*, 7322.

(74) Dallos, M.; Lischka, H.; Shepard, R.; Yarkony, D. R.; Szalay, P. G. *J. Chem. Phys.* **2004**, *120*, 7330.

(75) Barbatti, M.; Granucci, G.; Persico, M.; Ruckenbauer, M.; Vazdar, M.; Eckert-Maksic, M.; Lischka, H. *J. Photochem. Photobiol., A* **2007**, *190*, 228.

(76) Barbatti, M.; Granucci, G.; Lischka, H.; Ruckenbauer, M.; Persico, M. *NEWTON-X: a package for Newtonian dynamics close to the crossing seam*, version 0.14b, 2007, www.univie.ac.at/newtonx.

(77) Norton, J. E.; Houk, K. N. *Mol. Phys.* **2006**, *104*, 993.

(78) Groenhof, G.; Schafer, L. V.; Boggio-Pasqua, M.; Goette, M.; Grubmuller, H.; Robb, M. A. *J. Am. Chem. Soc.* **2007**, *129*, 6812.

(79) Groenhof, G.; Bouxin-Cademartory, M.; Hess, B.; deVisser, S. P.; Berendsen, H. J. C.; Olivucci, M.; Mark, A. E.; Robb, M. A. *J. Am. Chem. Soc.* **2004**, *126*, 4228.

(80) Worth, G. A.; Hunt, P.; Robb, M. A. *J. Phys. Chem. A* **2003**, *107*, 621.

(81) Vreven, D. L.; Welch, L.; Reichel, F. D. *Invest. Ophthalmol. Vis. Sci.* **1997**, *38*, 4221.

(82) Mathies, R. A.; Cruz, C. H. B.; Pollard, W. T.; Shank, C. V. *Science* **1988**, *240*, 777.

(83) Kandori, H.; Furutani, Y.; Nishimura, S.; Shichida, Y.; Chosrowjan, H.; Shibata, Y.; Mataga, N. *Chem. Phys. Lett.* **2001**, *334*, 271.

(84) Logunov, S. L.; Song, L.; ElSayed, M. A. *J. Phys. Chem.* **1996**, *100*, 18586.

(85) Govindjee, R.; Balashov, S. P.; Ebrey, T. G. *Biophys. J.* **1990**, *58*, 597.

(86) Mathies, R. A.; Kukura, P.; McCamant, D.; Yoon, S. *Abstr. Pap Am. Chem. Soc.* **2005**, *230*, U2779.

(87) Suzuki, T.; Callender, R. H. *Biophys. J.* **1981**, *34*, 261.

JP903329J